Hydrogen atom temperature measured with wavelength-modulated laser absorption spectroscopy in large scale filament arc negative hydrogen ion source

H. Nakano, S. Nishiyama, M. Goto, K. Tsumori, M. Kisaki, K. Ikeda, K. Nagaoka, M. Osakabe, Y. Takeiri, O. Kaneko, and K. Sasaki

Citation: AIP Conference Proceedings **1655**, 020018 (2015); doi: 10.1063/1.4916427
View online: http://dx.doi.org/10.1063/1.4916427
View Table of Contents: http://scitation.aip.org/content/aip/proceeding/aipcp/1655?ver=pdfcov
Published by the AIP Publishing

Hydrogen Atom Temperature Measured with Wavelength-Modulated Laser Absorption Spectroscopy in Large Scale Filament Arc Negative Hydrogen Ion Source

H. Nakano[1) a)], S. Nishiyama[2)], M. Goto[1)], K. Tsumori[1)], M. Kisaki[1)], K. Ikeda[1)], K. Nagaoka[1)], M. Osakabe[1)], Y. Takeiri[1)], O. Kaneko[1)], and K. Sasaki[2)]

[1]*National Institute for Fusion Science, 322-6 Oroshi-cho, Toki 5095292, Japan*
[2] *Graduate school of Engineering, Hokkaido University, Kita 13, Nishi 8, Kita-ku, Sapporo 0608628, Japan*

[a)]Corresponding author: nakano@nifs.ac.jp

Abstract. The velocity distribution function of hydrogen atoms is one of the useful parameters to understand particle dynamics from negative hydrogen production to extraction in a negative hydrogen ion source. Hydrogen atom temperature is one of the indicators of the velocity distribution function. To find a feasibility of hydrogen atom temperature measurement in large scale filament arc negative hydrogen ion source for fusion, a model calculation of wavelength-modulated laser absorption spectroscopy of the hydrogen Balmer alpha line was performed. By utilizing a wide range tunable diode laser, we successfully obtained the hydrogen atom temperature of ~3000 K in the vicinity of the plasma grid electrode. The hydrogen atom temperature increases as well as the arc power, and becomes constant after decreasing with the filling of hydrogen gas pressure.

INTRODUCTION

One of the issues of negative hydrogen ion source development is to enhance the negative hydrogen ion (H^-) current in stable operation [1-4]. Increases of source-plasma-generation power and introduced gas pressure of hydrogen molecular (H_2) enhance H^- density in the vicinity of the plasma grid electrode (PE) and the H^- current [5]. The high discharge power raises the heat load of the plasma generation chamber and increases electron which are extracted with H^- and causes other heat loads of extraction (EE), acceleration (AE) and grounded grid electrodes (GE). The introduced H_2 leaks to the beam extraction and acceleration region through PE apertures. The H^- beam collides with the leaked H_2. And the H^- beam current through GE decreases. Secondary particles birthing by the collisions produce heat loads of the grid electrodes. Efficient H^- production and beam extraction are important to develop the high performance negative hydrogen ion source.

Understanding a mechanism from H^- production to extraction as the beam in the negative hydrogen ion source especially in the vicinity of the PE contributes to the efficient H^- production and extraction. Studies to clarify the mechanism have been examined [6-8]. Regarding cesium seeded negative hydrogen ion source, it is considered that H^- is mainly produced on the PE surface and that the largest part of the extracted H^- beam is the surface produced H^-. The hydrogen atom (H^0) and the proton (H^+) are candidates for parent particles of surface produced H^-. The parent particles obtain electrons from the cesium covered PE surface whose work function becomes low due to the thin cesium layer. Conversion efficiency of H^- from H^0 and H^+ relays kinetic energies of H^0 and H^+ and incident angles to the PE. Velocity distribution functions of H^0 and H^+ are important not only to understand the mechanism from the H^- surface production to the beam extraction but also to improve the negative hydrogen ion source performance.

Regarding H^0, laser absorption spectroscopy of the Balmer alpha line is one of the methods to measure velocity distribution function along the laser line direction. Hydrogen atom temperature which is one of the indicators of the velocity distribution function can also be evaluated from Doppler broadening of the absorption spectrum. In the vicinity of the PE in large scale filament arc negative hydrogen ion source for fusion at the National Institute for

Fourth International Symposium on Negative Ions, Beams and Sources (NIBS 2014)
AIP Conf. Proc. 1655, 020018-1–020018-7; doi: 10.1063/1.4916427

Fusion Science [9], the absorption of the Balmer alpha line could not be detected by conventional laser absorption spectroscopy due to thin optical thickness and large background emission from filament and plasma. By adapting wavelength-modulated laser absorption spectroscopy (frequency-modulated spectroscopy) which is one of the high sensitive laser absorption spectroscopy, the absorption was able to be detected.

In this article, we show a model calculation of the wavelength-modulated laser absorption spectroscopy for the Balmer alpha line, a system of the wavelength-modulated laser absorption spectroscopy adapted to the large scale negative hydrogen ion source and evaluation of H^0 temperature.

MODEL CALCULATION OF WAVELENGTH-MODULATED LASER ABSORPTION SPECTROSCOPY FOR HYDROGEN BALMER ALPHA LINE

For the wavelength-modulated laser absorption spectroscopy for H^0 temperature measurement, the laser light wavelength λ is slowly swept more than the Doppler broadening around the hydrogen Balmer alpha line and is simaltaneously modulated rapidly for lock-in detection which is useful for signal to noise ratio (SN) from detected DC signal being insufficient. The signal is modulated with frequency $\omega = 2\pi f$ to be in low noise level frequency region of $1/f$ noise which is generated by an amplifier, detector, and other devices. Only the modulated frequency component can be obtained by phase sensitive detection and is demodulated into the original component with high SN, i.e., high sensitive detection becomes possible. The laser light wavelength modulation is the same as the laser light frequency $\nu = c/\lambda$ modulation. Here, the light frequency is modulated as $\nu(t) = \nu_0 + \nu_m \sin\omega t$, where c is light speed, ν_0 is central light frequency of modulation, and ν_m is frequency modulation depth of the light frequency. Transmitted light intensity $\tau(\nu(t))$ through the plasma becomes $\tau(\nu_0 + \nu_m \sin\omega t)$. If the frequency modulation depth ν_m is sufficiently smaller than ν_0, the Taylor expansion of transmitted light intensity yields,

$$
\begin{aligned}
\tau(\upsilon) &= \tau(\upsilon_0) + \sum_n \frac{\upsilon_m}{n!} \sin^n \omega t \left(\frac{d^n \tau(\upsilon)}{d\upsilon^n}\right)_{\upsilon_0} \\
&= \tau(\upsilon_0) + \left[\frac{\upsilon_m}{4}\left(\frac{d^2\tau}{d\upsilon^2}\right)_{\upsilon_0} + \frac{{\upsilon_m}^3}{64}\left(\frac{d^4\tau}{d\upsilon^4}\right)_{\upsilon_0} + \cdots\right] \\
&\quad + \left[\left(\frac{d\tau}{d\upsilon}\right)_{\upsilon_0} + \frac{{\upsilon_m}^2}{8}\left(\frac{d^3\tau}{d\upsilon^3}\right)_{\upsilon_0} + \cdots\right] \sin\omega t \\
&\quad + \left[-\frac{\upsilon_m}{4}\left(\frac{d^2\tau}{d\upsilon^2}\right)_{\upsilon_0} + \frac{{\upsilon_m}^3}{48}\left(\frac{d^4\tau}{d\upsilon^4}\right)_{\upsilon_0} + \cdots\right] \cos 2\omega t \\
&\quad + \left[-\frac{{\upsilon_m}^2}{24}\left(\frac{d^3\tau}{d\upsilon^3}\right)_{\upsilon_0} + \frac{{\upsilon_m}^4}{384}\left(\frac{d^5\tau}{d\upsilon^5}\right)_{\upsilon_0} + \cdots\right] \sin 3\omega t + \cdots \; .
\end{aligned}
\tag{1}
$$

The first term is dominant in each bracket, thus a component of nth order derivative of the transmitted (absorption) spectrum is dominant in nth order harmonic oscillation of the input laser modulation. Each order of harmonic oscillation can be obtained by phase sensitive detection, such as the lock-in amplifier. An entire spectrum of the nth order harmonic oscillation can be found by the central laser frequency sweeping. A spectrum of the nth order harmonic oscillation is called nf spectrum, e.g., 1f, 2f, 3f and 4f spectra. Figure 1 shows a conceptual diagram of wavelength-modulated laser absorption spectroscopy with model calculation of the hydrogen Balmer alpha line absorption. In the calculation, the absorption spectrum is calculated from Doppler broadened fine structure of Balmer alpha. Hydrogen atomic temperature is 3000 K, and a whole absorption spectrum roughly forms Gaussian. When the input light sinusoidally modulates with ω around inflection and the peak points of the absorption curve, oscillation frequency components of transmitted light are mainly ω and 2ω, respectively. The 1f spectrum is the most sensitive but it crosses zero at the absorption peak wavelength. The 2f signal is the second most sensitive, and has a peak at the original absorption peak wave length and opposite sign peaks at both side of the absorption peak.

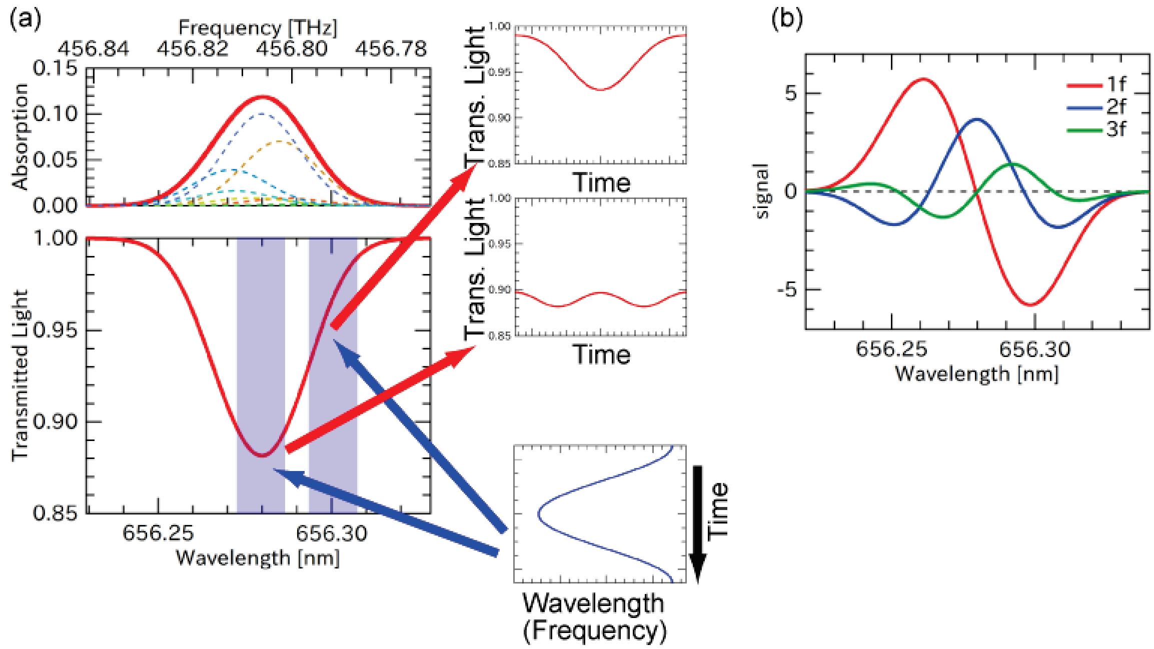

FIGURE 1. (a) Absorption and transmitted light spectra of hydrogen Balmer alpha at 3000 K of hydrogen atom temperature with examples of input wavelength modulation waveform and output one. (b) 1f, 2f and 3f signals of spectrum (a).

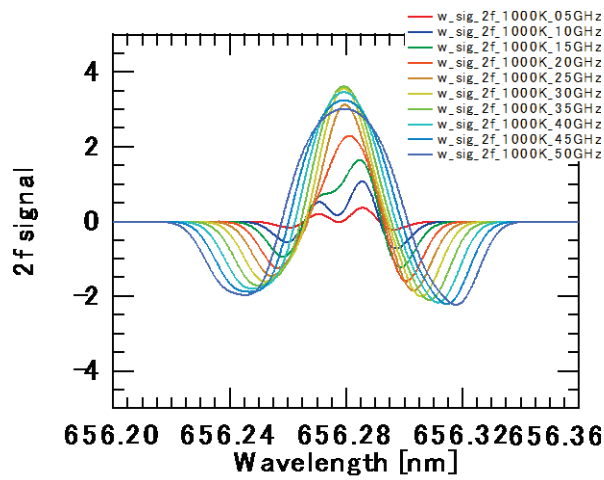

FIGURE 2. 2f signal calculation of the hydrogen absorption of Balmer alpha line. Hydrogen atom temperature is 1000 K.

Figure 2 shows dependences of sensitivity and wavelength resolution on the frequency modulation depth. Here, the H^0 temperature is 1000 K. Small frequency modulation depth makes high wavelength resolution and low sensitivity. Large modulation depth brings large peak in 2f spectrum although the peak height falls in too high modulation depth. Modulation depth has to be chosen by considering absorption peak width (Doppler broadening), absorption amount (optical thickness), and signal to noise ratio.

EXPERIMENTAL SETUP

Experiments were performed in the negative hydrogen ion source to develop sources of NBI on LHD [9]. The source plasma is generated by filament arc discharge. The short and long side widths and height of the arc chamber

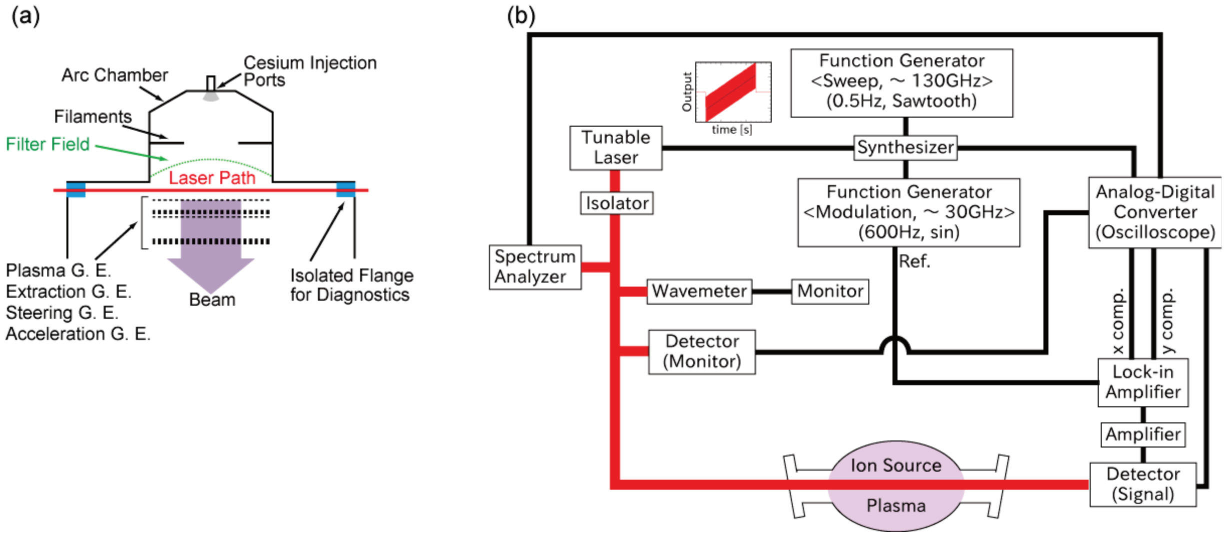

FIGURE 3. (a) Schematic view of the relation between laser and negative hydrogen ion source. (b) Experimental diagram of laser line and electric components.

are 0.35 m 0.70 m and 0.23 m, respectively. The plasma thickness of the short side width of 10 mm distant from the PE is defined as 0.18 m which is the full width at the half maximum of electron density profile measured with the Langmuir Probe.

The hydrogen Balmer alpha line laser is oscillated by a tunable diode laser. The nominal laser power is 18 mW with cw. The mode hop free range is 130 GHz which corresponds to 0.187 nm around 656.273 nm which is the nominal central calibrated wavelength. The laser light frequency was slowly swept with the laser frequency width of ~100 GHz (0.144 nm) at 0.5 Hz and simultaneously fast modulated with the 30 GHz (0.043 nm) sinusoidal wave at 600Hz. We selected 2f spectrum in this study in order to evaluate the absorption peak position and Doppler broadening. These can be estimated by wavelength widths between zero cross points and between two side peak positions of the central peak. The modulation depth of 30 GHz was decided from the central peak height of the 2f spectrum. Signals for wavelength sweep and modulation are produced by two function generators and are sent to a controller of the tunable diode laser after being combined by synthesizer. The fast oscillated signal is transferred to the lock-in amplifier as reference signal. A part of the laser light oscillated from the laser head is carried to the Fabry-Perot interferometer type spectrum analyzer and wave meter. The main part of the laser light is injected in to the arc chamber in the direction of short side width and to the plasma in the vicinity (~10 mm) of the PE through a tilted window mounted at the bias insulator placed between the arc chamber flange and the PE flange. Output laser through the opposite side tilted window is detected by photodiode detector. The detected signal is transferred to the lock-in amplifier. To obtain good signal to noise ratio from one output signal from the lock-in amplifier, a phase between the detected signal and the reference signal is calibrated as in-phase (x comp. in Fig. 3(b)) or quadrature (y comp.) components of the second harmonic oscillation are minimized. Another component is mainly utilized for

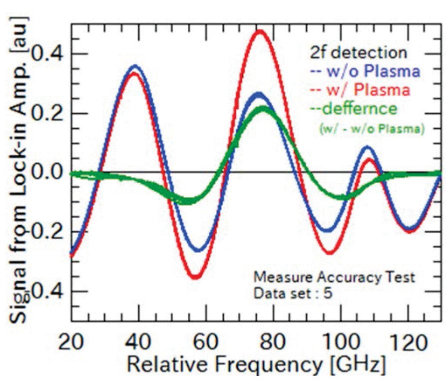

FIGURE 4. Experimental data of 2f signal.

analysis. An analog-digital converter preserves the detected signal of the laser, the in-phase and quadrature components, the function generator signals, and the spectrum analyzer signal.

HYDROGEN TEMPERATURE IN THE VICINITY OF PLASMA ELECTRODE

The 2f spectrum is derived as a signal difference of the lock-in amplifier between with and without plasmas. Figure 4 shows five sets of measured in-phase signals with and without plasmas, and five 2f spectra calculated from the five sets. The plasmas were generated with 50 kW of input arc power and 0.3 Pa introduced hydrogen gas

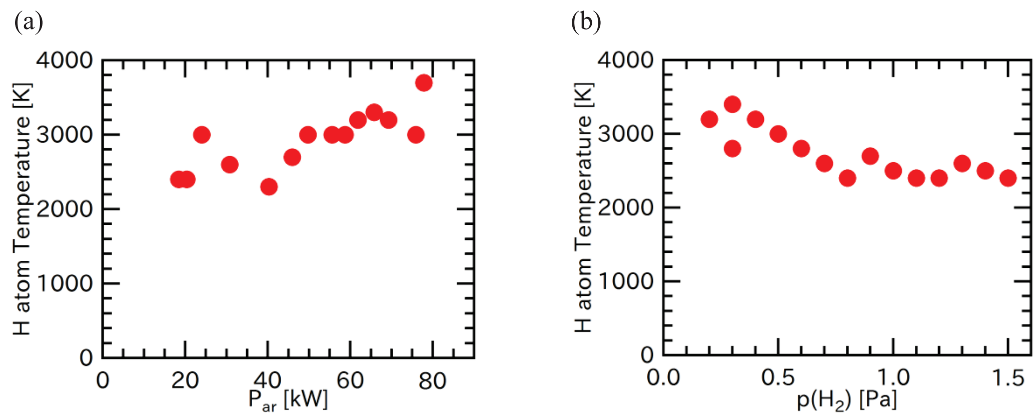

FIGURE 5. Hydrogen atom temperature in the discharge without cesium as the functions of with (a) input arc power and (b) introduced hydrogen gas pressure in the arc chamber.

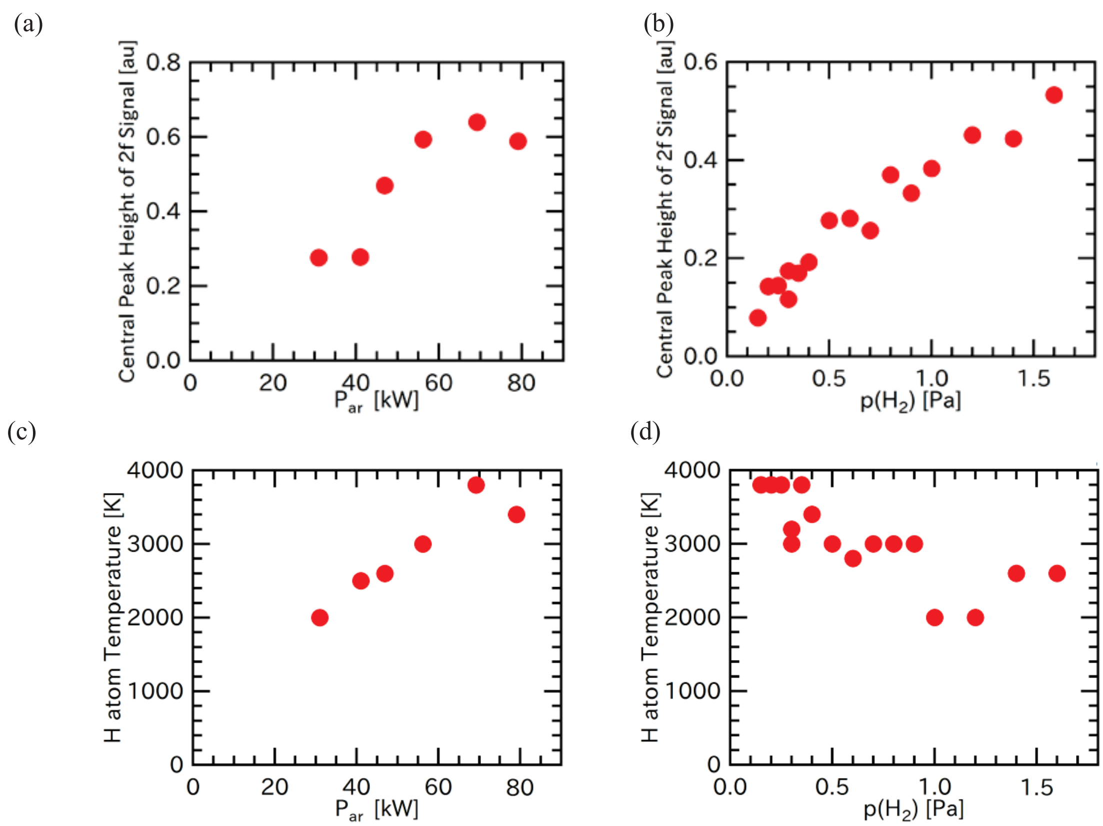

FIGURE 6. Central peak height of 2f signal as the functions of (a) input arc power and (b) introduced hydrogen gas pressure. Hydrogen atom temperature in the discharge with cesium as the functions of with (c) input arc power and (d) introduced hydrogen gas pressure in the arc chamber.

pressure without cesium seeding. Good experimental reliability was performed and measure accuracy corresponds to line thickness. Obtained 2f spectra were compared to the model calculation spectrum using temperature step of 100 K especially with attention of the wavelengths of zero cross, the central absorption peak and the opposite side peaks. The H^0 temperature is evaluated with ~3000 K including ~200 K uncertainty. This value is similar to previous study [10]. In no cesium seeded plasmas where introduced hydrogen gas pressure is 0.3 Pa, the H^0 temperature weakly increases in the range of 2400 K to 3500 K with input arc power in the range of 20 kW to 80 kW (Fig. 5 (a)). With respect to introduced hydrogen gas pressure, the H^0 temperature decreases to 2200 K from 3400 K by 0.8 Pa in the plasmas where input arc power are 50 kW (Fig. 5 (b)). In the higher introduced hydrogen gas pressure, the H^0 temperature is constant.

In the cesium seeded plasma, central peak height of 2f signal and H^0 temperature as functions of input arc power and introduced hydrogen gas pressure are shown in Fig. 6. Increase of the central peak height of 2f signal with the input arc power means dissociation degree n_H/n_{H2} rises with the input arc power. Here the values n_H and n_{H2} are atomic and molecular hydrogen densities, respectively. A linear relation between the central peak height and introduced hydrogen gas pressure represents constant value of n_H/n_{H2}. Decrease of the absorption amount was found in the cesium seeded plasma. In the vicinity of the PE in the cesium seeded plasma, the number of the electron impact excitation to n = 2 state of H^0 decreases due to electron density becoming very low. Although n = 2 state of H^0 produced by mutual neutralization ($H^- + H^+ \rightarrow H^0(1s) + H^0(n=2)$) may increase because of increased H^- density, a tendency of the relation between the H^0 temperature with input arc power and introduced hydrogen gas pressure and absolute H^0 temperature in cesium seeded plasma is similar to that in the plasma without cesium. These results mean that the H^0 temperature depends upon the discharge parameter in the plasma generation region (driver region) and most of the n = 2 state H^0 produced in the plasma generation region.

CONSIDERATIONS

In the source plasma where the electron temperature is several eV, it is considered that the initial energetic H^0 is mainly generated by dissociation of the H_2 molecules of the Franck-Condon process. The initial energy of H^0 is ~3 eV. In the vicinity of the PE, the electron temperature decreases to less than 1 eV by filter and electron deflection magnetic fields traversing the beam axis. Therefore the Franck-Condon process mainly occurs in the driver region. The measured H^0 temperature ~ 3000 K (~ 0.3 eV) is the bulk component parallel and perpendicular to the PE and the beam axis, respectively. The energetic H^0 is thermalized by collisions with induced hydrogen gas molecules and the walls, and by recombination processes until coming to the vicinity of the PE.

The minimum work function of molybdenum PE covered by thin cesium layer is ~ 1.6 eV. Electron affinity level of a negative hydrogen ion is 0.75 eV. The threshold kinetic energy of H^0 to produce the negative hydrogen ion on the PE becomes ~ 0.85 eV which is approximate three times higher than H^0 thermal energy. Most of the thermalized bulk part does not affect the negative hydrogen ion production on the PE, although the high energy part of ~ 0.1 % in thermalized H^0 component may provide influence. If the H^0 density in the vicinity of the PE is the order of 10^{19} m^{-3} which is the hydrogen molecular density in filling pressure of 0.3 Pa, the high energy part of H^0 becomes 10^{16} m^{-3}. This is lower than the measured negative hydrogen ion density of 10^{17} m^{-3}. The production amount of H^- cannot be explained by the Doppler broadening of H^0. One of the candidates to explain the H^- density is that high energy H^+ exists in quantity and mainly contributes the H^- surface production. Another possibility to enhance H^- surface production is the plasma flow including H^0 with kinetic energy of ~ 1 eV perpendicular to the PE from driver region to the PE. A H^0 density evaluation and measurement of the plasma flow are future studies.

CONCLUSION

The model calculation of the wavelength-modulated laser absorption spectroscopy for n = 2 state of H^0 was performed. When the H^0 temperature is 3000 K, most of 1f, 2f and 3f spectrum shapes are less than 0.12 nm and ~656.28 nm. The modulation depth for the H^0 temperature range of some 1000 K needed to be optimized from some 0.01 nm (some tens of GHz) range of light wavelength (frequency) by signal sensitivity and the wavelength resolution. The wavelength-modulated laser absorption spectroscopy was applied for H^0 temperature measurement in large scale filament arc negative hydrogen ion source for fusion. Good reproducibility data were obtained by the tunable diode laser with wide range wavelength sweep as more than 0.12 nm. The H^0 temperature increase from 2400 K to 3500 K as well as the arc power from 20 kW to 80 kW in the no cesium seeded plasma where the introduced hydrogen gas pressure is 0.3 Pa. Regarding introduced H_2 pressure, the H^0 temperature decreased to 2200

K from 3400 K by 0.8 Pa and is almost constant up to 1.5 Pa. The tendency and absolute value of the H^0 temperature in the plasma without cesium are similar to those with cesium. The plasma parameters in the driver region strongly affect the H^0 temperature in the plasma whether without cesium or with cesium.

Most H^0 with 3000 K cannot produce H^- on the cesium seeded PE. To explain measured density of H^- whose parent particle is H^0, the H^0 density in the vicinity of the PE needs higher order of magnitude than electron density of 10^{18} m^{-3} in the driver region. Another possibility is that the flow of H^0 and/or H^+ to the PE exit. Absolute value estimation of H^0 and observation of the flows are forthcoming challenges.

ACKNOWLEDGMENTS

This research is supported by the NIFS Collaboration Research Program NIFS13KLER021, NIFS Research Programs NIFS13ULRR008 and NIFS13ULRR702, and JSPS KAKENHI Grant Numbers 25800307, 25249134.

REFERENCES

1. R. Hemsworth, H. Decamps, J. Graceffa, B. Schunke, M. Tanaka, M. Dremel, A. Tanga, H.P.L. De Esch, F. Geli, J. Milnes, T. Inoue, D. Marcuzzi, P. Sonato, and P. Zaccaria, Nucl. Fusion **49**, p. 045006 2009.
2. A. Kojima, M.Hanada, Y. Tanaka, T. Inoue, K. Watanabe, M. Taniguchi, M. Kashiwagi, N. Umeda, H. Tobari, L. R. Grisham and JT-60 NBI Group, Rev. Sci. Instrum. **81**, 02B112 (2010).
3. Y. Takeiri, K. Tsumori, K. Ikeda, M. Osakabe, K. Nagaoka, Y. Oka, E. Asano, T. Kondo, M. Sato, M. Shibuya, S. Komada, and O. Kaneko, AIP Conf. Proc. **1097**, pp. 470-479, 2009.
4. H. Oguri, A. Ueno, K. Ikegami, Y. Namekawa, and K. Ohkoshi, Physical Review Special Topics-Accelerators and Beams **12**, 010401 (2009).
5. H. Nakano, K. Tsumori, K. Nagaoka, M. Shibuya, U. Fantz, M. Kisaki, K. Ikeda, M. Osakabe, O. Kaneko, E. Asano, T. Kondo, M. Sato, S. Komada, H. Sekiguchi and Y. Takeiri, AIP Conf. Proc. **1390**, 359 (2011).
6. H. Nakano, K. Tsumori, M. Kisaki, K. Ikeda, K. Nagaoka, M. Osakabe, O. Kaneko, E. Asano, T. Kondo, M. Sato, M. Shibuya, S. Komada, H. Sekiguchi and Y. Takeiri, AIP Conf. Proc. **1515**, 237 (2013)
7. H. Nakano,K. Tsumori, K. Ikeda, M. Kisaki, M. Shibuya, K. Nagaoka, M. Osakabe, E. Asano, T. Kondo, M. Sato, S. Komada, H. Sekiguchi, Y. Takeiri, O. Kaneko, *15th International Conference on Ion Source,* 9th – 13th September 2013*,* TueP74, Chiba, Japan.
8. Y. Takeiri, K. Tsumori, K. Ikeda, H. Nakano, M. Kisaki, K. Nagaoka, T. Tokuzawa, S. Geng*, M. Osakabe, O. Kaneko, T. Kondo, M. Sato, M. Shibuya, S. Komada, and H. Sekiguchi, *4th International Symposium on Negative Ions, Beams and Sources*, 6th – 10th October 2014, O4-01, Garching, Germany.
9. K. Tsumori, Y. Takeiri, O. Kaneko, M. Osakabe, A. Ando, K. Ikeda, K. Nagaoka, H. Nakano, E. Asano, M. Shibuya, M. Sato, T. Kondo and M. Komada, J. Fusion Sci. Technol. **58**, pp. 482-488, 2010.
10. A. M. Bruneteau, G. Hollos, M. Bacal, and J. Bretagne, J. of Appl. Phys. **67**, 7254 (1990).